Available online at www.sciencedirect.com
ScienceDirect
Journal of Power Sources 158 (2006) 914–919
JOURNAL OF POWER SOURCES
www.elsevier.com/locate/jpowsour

Short communication

Electrochemical behavior of lead alloys in sulfuric and phosphoric acid electrolyte

S. Li [a], H.Y. Chen [a,*], M.C. Tang [b], W.W. Wei [b], Z.W. Xia [b], Y.M. Wu [b], W.S. Li [a], X. Jiang [a]

[a] *School of Chemistry and Environment, South China Normal University, Guangzhou, Guangdong 510631, China*
[b] *Zhuzhou Smelter Group Co. Ltd., Zhuzhou, Hunan 412004, China*

Available online 28 December 2005

Abstract

The electrochemical behavior of lead, lead–calcium–tin–aluminum and lead–calcium–tin–aluminium–bismuth alloy electrode has been studied in the electrolyte of sulfuric, phosphoric and mixed acid electrolyte. The electrochemical measurements were performed using a cyclic voltammetry technique (CV) with three-electrode system. The results demonstrated that bismuth(III) doped in the lead electrode can increase electrical capacity. The oxidation peak potential of lead alloy electrode in phosphoric acid shifted to the positive compared to that in sulfuric acid. The formation of $PbHPO_4$ in phosphoric acid and its passivation are responsible for the positive shift of the oxidation.

Keywords: Lead-acid battery; Lead alloy electrode; Bismuth; Phosphoric acid; Cyclic voltammetry technique (CV); Anodic oxidation

1. Introduction

Phosphoric acid has been used as an additive to lead-acid batteries since 1920 [1], which can reduce the sulfation (especially in the deep-discharge state) and increase cycle life by reducing the shedding of positive active material [2,3]. On the other hand, adverse effects of phosphoric acid have also been studied, including the capacity loss in the initial cycles, excessive mossing, and poor temperature performance.

Bullock [4–6] proposed that phosphate could be adsorbed reversibly on the surface of PbO_2 during charge process and could improve the crystal growth of PbO_2 on the lead grid, and avoid readily discharging to $PbSO_4$. The formation of $Pb_3(PO_4)_2$ as an intermediate in the corrosion process from Pb to PbO_2 was regarded as an important function of H_3PO_4 in lead-acid batteries. Garche et al. [7] found that the reduction of the capacity but the improvement of lifetime under deep-discharge service seem to originate from the considerable decrease of the crystal size of $PbSO_4$ in the presence of phosphoric acid, whereas the $PbSO_4$ protects the corrosion layer against further discharge. Dōring and Wiesener [8] observed that phosphate ions adsorbed specifically on lead dioxide influence nucleation and nuclei growth of PbO_2. Venugopalan [9] found H_3PO_4 limits significantly the adverse effect of antimony in lead alloy, and H_3PO_4 was also found to increase the hydrogen over-potential without negative effect on $Pb/PbSO_4$ reaction. Sternberg et al. [10] showed the addition of H_3PO_4 passivates strongly all the electrode process, and phosphoric acid increase the oxygen over-potential. As suggested by Chatelut et al. [11], the increases of the electrical charge Q_a during the oxidation process and the charges of reduction are due to changes in the surface morphology. Paleska et al. [12] suggested the fact that quasi-reversible surface processes of lead during cyclic polarization in sulfuric and phosphoric acids lead to changes of the roughness factor and to incomplete reduction of the oxidant formed on the electrode surface.

The research and discussion on the mechanism in the presence of the bismuth in alloys has been investigated for a long time [13–15], but the electrochemical behavior of lead–calcium–tin–aluminum in the presence of bismuth has not been studied in detail. Because gelled lead-acid batteries become popular nowadays, Pb and Pb/PbO electrodes have been widely studied in H_2SO_4 solution, but only H_3PO_4 and mixed acid (H_2SO_4 and H_3PO_4) have been studied as the addition [11]. As far as we know, the electrochemical behavior of lead–calcium–tin–aluminum–bismuth alloy in the phosphoric acid solutions with various concentrations has not been reported previously.

The electrode behavior of lead, lead–calcium–tin–aluminum, lead–calcium–tin–aluminum–bismuth alloys in sulfuric and

* Corresponding author. Tel.: +86 20 3931 0183; fax: +86 20 3931 0187.
E-mail address: battery@scnu.edu.cn (H.Y. Chen).

0378-7753/$ – see front matter © 2005 Elsevier B.V. All rights reserved.
doi:10.1016/j.jpowsour.2005.11.028

phosphoric acid solutions were studied in the paper, the influence of phosphoric acid as an addition to electrolyte was also discussed in detail.

2. Experimental

The lead alloy rods were taken as working electrodes in the experiment, including Pb–Ca–Sn–Al (0.12% Ca, 0.82% Sn, 0.026% Al; 0.3 cm^2 of geometric area) and Pb–Ca–Sn–Al–Bi (0.12% Ca, 0.82% Sn, 0.026% Al, 0.05% Bi; 0.3 cm^2 of geometric area) alloys. The oxide and carbonate layer were eliminated by polishing the electrode with abrasive papers (500#, 800#, 1200#, 1500#, 2000#) in turn before the experiment, the electrode was then quickly washed with deionized water and put into use immediately.

The experiments were performed in the electrolyte of sulfuric acid solution (1.28 M), phosphoric acid solution with various concentrations (0.52, 1.11, 1.65, 2.30, and 2.90 M) and the mixed acids (1.28 M sulfuric acid/1.65 M phosphoric acid), H_2SO_4 and H_3PO_4 were of analytical grade.

Cyclic voltammetry was performed with Autolab PGSTAT-30 potentionstat/galvanostat (ECO Echemie B.V., Holland) at scan rates ranging from 5 to 50 mV s^{-1}. Usually, the potential of the pure lead and lead alloy electrodes was cycled in the range −1.3 to −0.7 and 0.5–1.4 V, the platinum foil and the Hg/Hg_2SO_4 electrode were used as the counter and reference electrode, respectively. The experiments were carried out at room temperature (298 K).

3. Results and discussion

3.1. Electrochemical behavior of Pb–Ca–Sn–Al–Bi alloy electrode in aqueous sulfuric acid/aqueous phosphoric acid/gelled phosphoric acid electrolyte

Fig. 1 shows cyclic voltammetric curves of lead electrodes in gelled phosphoric electrolyte at 20 mV s^{-1}, and Table 1 lists parameters of cyclic voltammetry of lead electrodes in gelled phosphoric at 20 mV s^{-1}. As shown in Table 1, the rest potentials of lead electrodes were identical, and the anodic oxidation current of lead alloy electrode containing bismuth was higher than that of pure lead electrode, moreover the anodic oxidation peak potential of lead alloy electrode containing bismuth shifted 169.7 mV towards positive direction. The results suggest the first solution of lead in alloy electrode, and the anodic oxidation of lead to phosphate (Pb → Pb(II)) is more difficult for the lead alloy electrode containing bismuth than the pure lead electrode in phosphoric acid.

Table 1
Parameters of cyclic voltammetry for lead electrodes in gelled phosphoric and aqueous sulfuric acid electrolyte at 20 mV s^{-1}

Electrode	Gelled phosphoric electrolyte		
	$I_{p,a}$ (mA)	$E_{p,a}$ (V)	Rest potential (V)
Pb–Ca–Sn–Al–Bi	8.6	−0.63	−0.92
Pb–Ca–Sn–Al	7.8	−0.63	−0.92
Pb	3.9	−0.80	−0.93

To further understand whether the intermingling of bismuth in Pb–Ca–Sn–Al alloy electrode lead to the charge change of anodic oxidation, voltammetry has been performed in aqueous phosphoric acid (Fig. 2) and in aqueous sulfuric acid electrolyte (Fig. 3), respectively. The relative parameters of cyclic voltammetry in Figs. 2 and 3 are shown in Table 2.

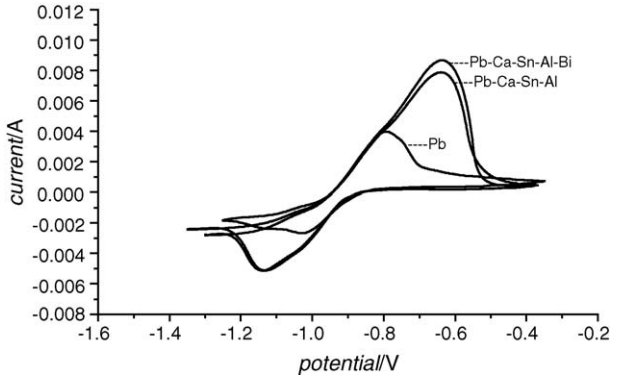

Fig. 1. Cyclic voltammetric curves of Pb electrodes in gelled phosphoric electrolyte at 20 mV s^{-1}.

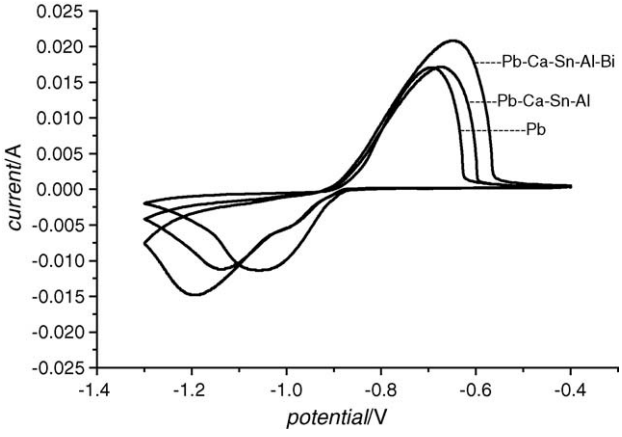

Fig. 2. Cyclic voltammetric curves of lead electrodes in aqueous phosphoric acid electrolyte at 20 mV s^{-1}.

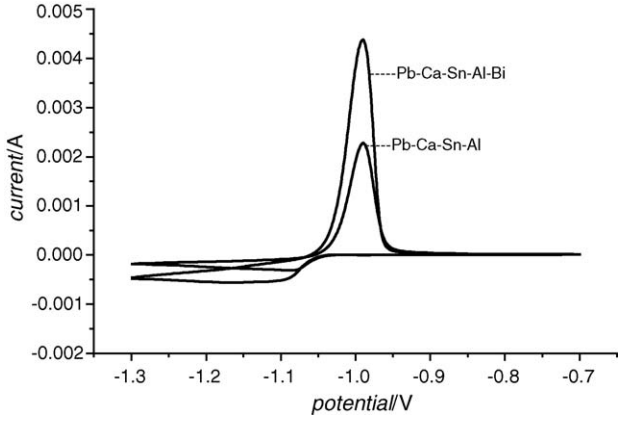

Fig. 3. Cyclic voltammetry curves of lead electrodes in aqueous sulfuric acid electrolyte at 20 mV s^{-1}.

Table 2
Parameters of cyclic voltammetry for lead electrodes in aqueous phosphoric electrolyte and sulfuric acid electrolyte at 20 mV s^{-1}

Electrode	Aqueous phosphoric electrolyte			Aqueous sulfuric acid		
	$I_{p,a}$ (mA)	$E_{p,a}$ (V)	Rest potential (V)	$I_{p,a}$ (mA)	$E_{p,a}$ (V)	Rest potential (V)
Pb–Ca–Sn–Al–Bi	15	−0.69	−0.90	4.2	−0.99	−1.04
Pb–Ca–Sn–Al	15	−0.67	−0.93	2.2	−0.99	−0.93
Pb	19.5	−0.64	−0.92			

Similarly, the anodic oxidation peaks of cyclic voltammetry of three kinds of electrodes in aqueous phosphoric acid electrolyte in Fig. 2 show the same characteristic as in gelled phosphoric electrolyte, the anodic oxidation current of lead alloy electrode containing bismuth in aqueous phosphoric acid was higher than that of lead electrode without bismuth, moreover the anodic oxidation peak potential of lead alloy electrode containing bismuth in aqueous phosphoric acid shifted 51 mV towards positive direction than that of pure lead electrode. More negative cathodic reduction peak of Pb–Ca–Sn–Al electrode suggests that Pb(II) in electrolyte is more difficult to reduce to lead.

Fig. 3 shows cyclic voltammetry curves of lead electrodes in aqueous sulfuric acid electrolyte at 20 mV s^{-1}, which are different from those in phosphoric acid. In an experimental potential range from −1.3 to −0.7 V, no other peak appears except anodic oxidation peak of Pb–Ca–Sn–Al–Bi electrode, which is identical with that of lead alloy electrode without bismuth. But the rest potential of the Pb–Ca–Sn–Al–Bi electrode showed more negative value (less 115 mV than that of Pb–Ca–Sn–Al electrode), and the oxidation peak current of the Pb–Ca–Sn–Al–Bi electrode is higher than that of Pb–Ca–Sn–Al electrode shown in Table 1. The result suggests that bismuth in the lead alloy electrode in sulfuric acid does not take part in electrochemical reaction, but bismuth can promote the oxidation reaction and lead to the increase oxidation peak current. The porosity-producing effect of bismuth in cathode should probably be the main cause that leads to the capacity increase in lead-acid battery. Bi_2O_3 as an alkaline oxidant comes into being on the alloy electrode, then dissolves in aqueous sulfuric and phosphorus solution, and apertures lead to the increase of oxidation peak current, which is shown in the cyclic voltammetric curves in Figs. 1–3.

3.2. The anodic oxidation of Pb–Ca–Sn–Al electrode in phosphoric acid

The oxidation peak potential of three kinds of electrodes in gelled and aqueous phosphoric acid solution shows more positive value than in sulfuric acid, whereas the phenomenon does not occur in sulfuric acid (Fig. 4). To further understand whether phosphoric acid will lead to the positive shift of the oxidation peak potential, the cyclic voltammetric curves of Pb–Ca–Sn–Al electrode were compared in aqueous phosphoric acid, aqueous sulfuric acid and mixed phosphoric–sulfuric acid in Figs. 5 and 6, and parameters of the voltammetry are listed in Table 3. It can be seen from Table 3, the oxidation peak potential of Pb–Ca–Sn–Al electrode in aqueous phosphoric acid shifted 344.8 mV towards the positive direction, and the rest potential is 138.5 mV. The

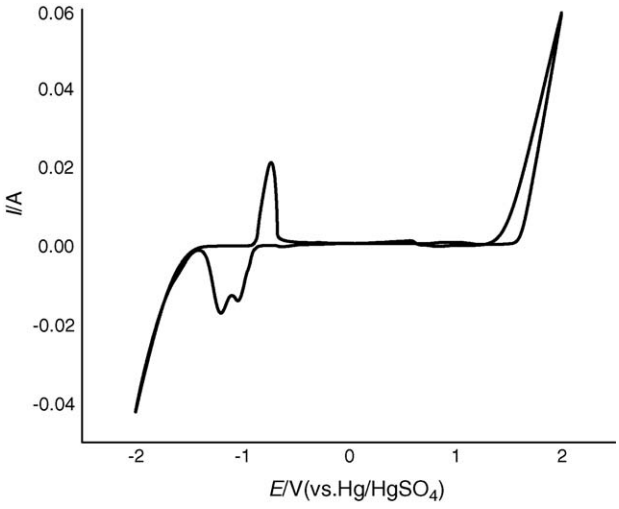

Fig. 4. Cyclic voltammetric curves of Pb–Ca–Sn–Al electrode in aqueous phosphoric acid electrolyte at 10 mV s^{-1}.

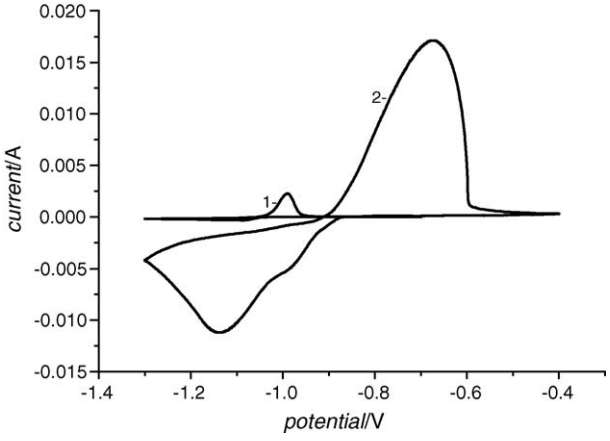

Fig. 5. Cyclic voltammetric curves of Pb–Ca–Sn–Al electrode in aqueous phosphoric acid electrolyte (1) and aqueous sulfuric acid electrolyte (2) at 20 mV s^{-1}.

results suggested that it is difficult for lead to reduce to Pb(II) in phosphoric acid. On the other hand, the oxidation peak current in aqueous sulfuric acid is higher than that in aqueous phosphoric acid of 15.6 mA.

Table 3
Parameters of cyclic voltammetry for lead–calcium electrode in phosphoric, sulfuric and mixed acid electrolytes at 20 mV s^{-1}

Electrolyte	$I_{p,a}$ (mA)	$E_{p,a}$ (V)	Rest potential (V)
Phosphoric acid	2.09	−0.645	−0.9074
Sulfuric acid	4.32	−0.9898	−1.045
Mixed acid	2.8	−0.9979	−1.046

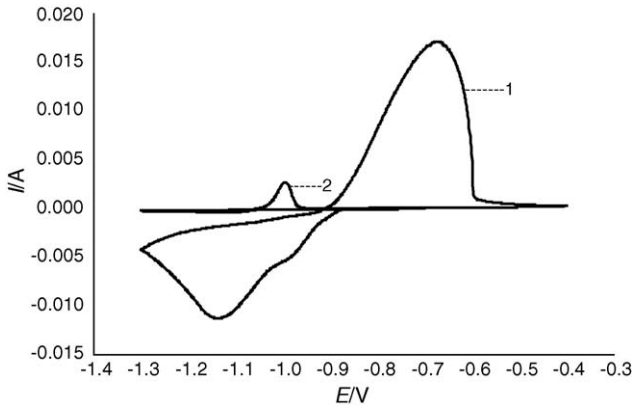

Fig. 6. Cyclic voltammetric curves of Pb–Ca–Sn–Al electrode in phosphoric acid electrolyte (1) and mixed acid electrolyte (2) at 20 mV s^{-1}.

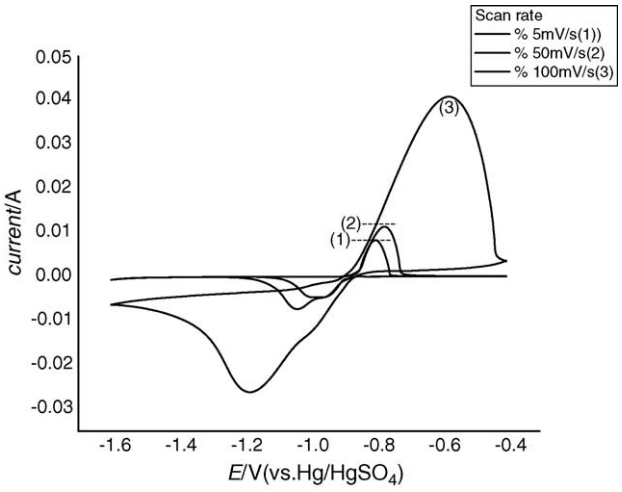

Fig. 7. Cyclic voltammograms of Pb–Ca–Sn–Al electrode in 1.65 M H_3PO_4 at different scan rates.

The same rest potentials of Pb–Ca–Sn–Al electrode were observed in sulfuric and mixed acid, but the more negative oxidation peak potential and the smaller current were shown in the CV curves of mixed acid in sulfuric acid. This phenomenon can be explained as follows.

Firstly, The oxidation peak potential of lead alloy electrode in phosphoric acid shows more positive than that in sulfuric acid, the $PbHPO_4$ [10,11] formed in phosphoric acid will cover the surface of the lead electrode and lead to its passivation and oxidation peak potential shift towards positive direction, relative reaction is listed as follows:

$$Pb \rightarrow Pb^{2+} + 2e^- \quad (1)$$

$$Pb^{2+} + HPO_4{}^{2-} = PbHPO_4 \quad (2)$$

Secondly, as a porous material, $PbHPO_4$ is less compact than $PbSO_4$. The increasing porosity is beneficial for the diffusion of phosphoric acid electrolyte to the inner of active material. As a result, the acidity in the space of active material in the plate containing bismuth is higher when the more β-PbO_2 occurs. Here β-PbO_2 with tiny crystalline grains shows high discharge capacity.

Two kinds of sediments appeared simultaneously in the mixed acid including 1.65 M H_3PO_4, but $PbHPO_4$ probably was the main product and responsible for the negative potential shift of anodic oxidation peak.

3.3. Electrochemical behavior of Pb–Ca–Sn–Al–Bi alloy electrode in phosphoric acid

In order to study the effect of the phosphoric acid on the active material in lead-acid battery, the cyclic voltammetry of Pb–Ca–Sn–Al–Bi alloy electrode in phosphoric acid solution with different concentration were performed at different scan rates.

Fig. 7 shows the cyclic voltammograms of Pb–Ca–Sn–Al electrode in 1.65 M H_3PO_4 at different scan rates. It has been seen that the anodic oxidation peak moved to more positive potential and the peak current increased greatly with the increase of scan rate, and $Q_a/Q_c \neq 1$. The results suggested that the electrode reaction of lead alloy during cyclic voltammograms in sulfuric and phosphoric acids was not fully reversible, and the roughness factor or incomplete reduction of the oxidation compounds formed on the electrode surface led to such irreversibility of the reaction.

Fig. 8 shows cyclic voltammograms of Pb–Ca–Sn–Al electrode in 1.65 M H_3PO_4 at different scan rates. The same conclusion as below can be drawn from cyclic voltammograms of Pb–Ca–Sn–Al–Bi electrode in 1.65 M H_3PO_4 at different scan rates in Fig. 9.

Noticeably, there are two cathodic reduction peaks in a potential range from −1.5 to −0.9 V. A smaller cathodic reduction peak appeared in the more positive potential range. The smaller peak is not clear with large scan rate like 100 mV, and which is clear and close to the bigger peak with slow scan rate like 5 mV. Few papers reported the forming mechanism of this smaller peak that needs further study.

Fig. 9 shows CV curves of Pb–Ca–Sn–Al–Bi electrode in phosphoric acid with different concentration at 20 mV s^{-1}. The anodic oxidation peak shifted to the positive potential and peak

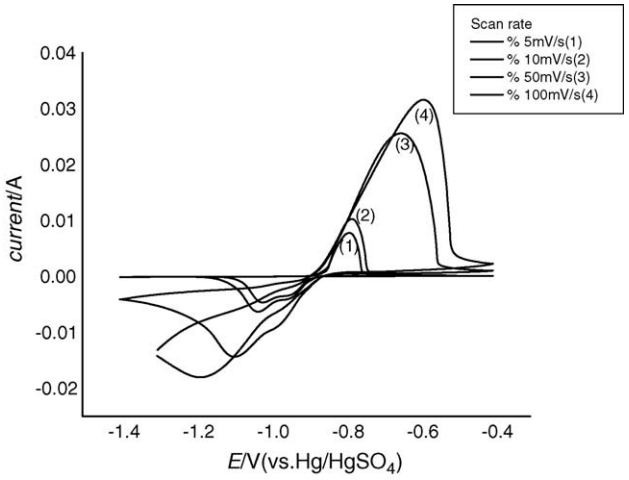

Fig. 8. Cyclic voltammograms of Pb–Ca–Sn–Al–Bi electrode in 1.65 M H_3PO_4 at different scan rates.

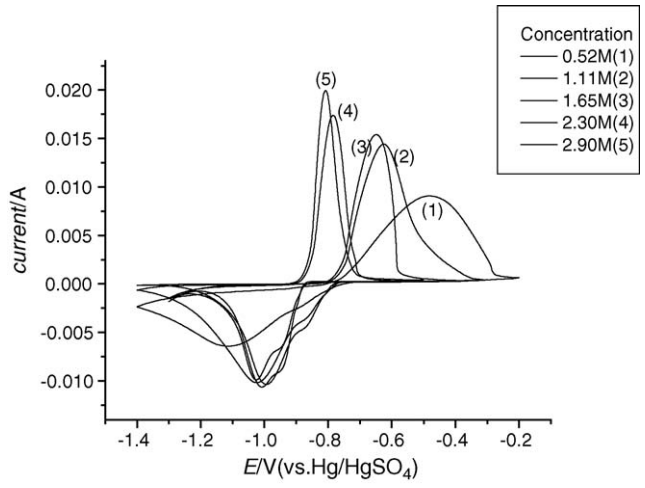

Fig. 9. Voltammograms of Pb–Ca–Sn–Al–Bi electrode in H_3PO_4 with different concentration at 20 mV s^{-1}.

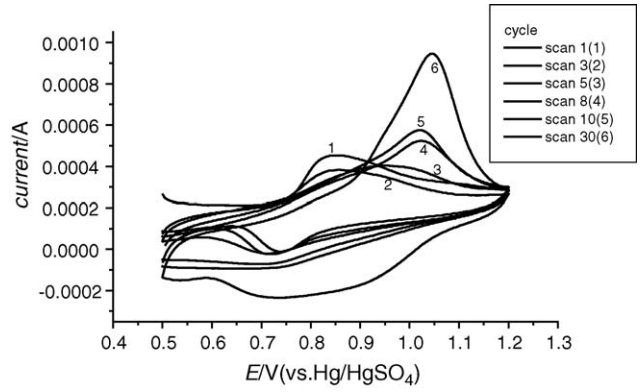

Fig. 10. The CV curves of Pb–Ca–Sn–Al–Bi electrode in 1.65 M.

current decreased with the reduction of phosphoric acid concentration. E_p and i_p of the bigger cathodic reduction peaks of phosphoric acid were same with the different concentration, but E_p of the smaller peaks shifted to the negative with the reduction of the H_3PO_4 concentration.

The CV curves of Pb–Ca–Sn–Al–Bi electrode in 1.65 M at 5 mV s^{-1} are shown in Fig. 10. The anodic reduction peak potential moved to the more positive potential (0.84–1.05 V) and the peak current increased with increasing scan numbers, which suggested that the surface of the electrode became passivated. On the other hand, cathodic reduction peak disappeared after several cycles. Fig. 11 shows the dependence of Q_a and Q_c (charges of the anodic and cathodic process), obtained at 5 mV s^{-1}, on a number of scans for Pb–Ca–Sn–Al–Bi electrode in 1.65 M H_3PO_4 (Table 4).

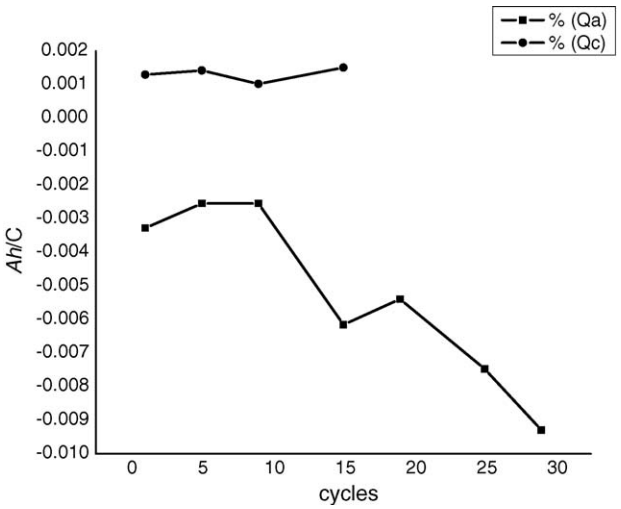

Fig. 11. The dependence of Q_a and Q_c, obtained at 5 mV s^{-1} on a number of scans for Pb–Ca–Sn–Al–Bi electrode in 1.65 M H_3PO_4.

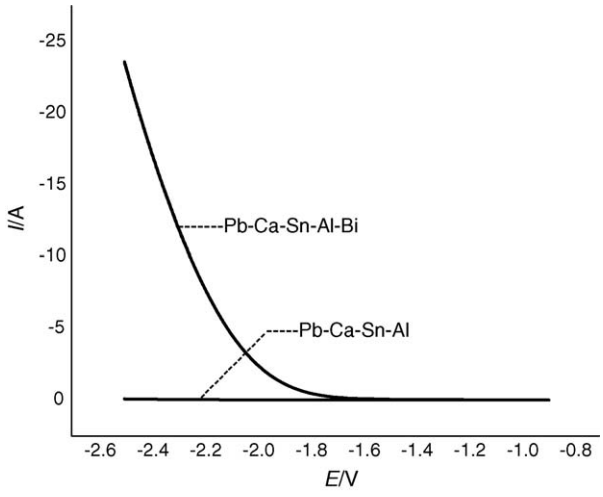

Fig. 12. Steady cathodic polarization curves of Pb–Ca–Sn–Al and Pb–Ca–Sn–Al–Bi electrodes in 1.65 M H_3PO_4

3.4. Hydrogen evolution of Pb–Ca–Sn–Al and Pb–Ca–Sn–Al–Bi alloys in aqueous phosphoric acid solutions

Fig. 12 shows steady cathodic polarization curves of Pb–Ca–Sn–Al and Pb–Ca–Sn–Al–Bi electrodes in 1.65 M H_3PO_4 solution. The hydrogen evolution current of Pb–Ca–Sn–Al–Bi electrode was much larger than that of Pb–Ca–Sn–Al electrode. It indicated the hydrogen evolution easily occurred in Pb–Ca–Sn–Al–Bi electrode. The over-potential is logarithmic to the current at high over-potential as follows:

Table 4
Comparison of the oxidation charges (Q_a) of anodic peak a in cyclic voltammograms for Pb–Ca–Sn–Al–Bi electrode in 1.65 M H_3PO_4 at 5 mV s^{-1}

	Scan 1	Scan 2	Scan 3	Scan 5	Scan 8	Scan 10
Q_a ($\times 10^{-4}$ C)	321.6	290.6	314.6	373.6	384.4	453.4
$E_{p,a}$ (V)	0.838	0.836	0.937	1.017	1.023	1.04

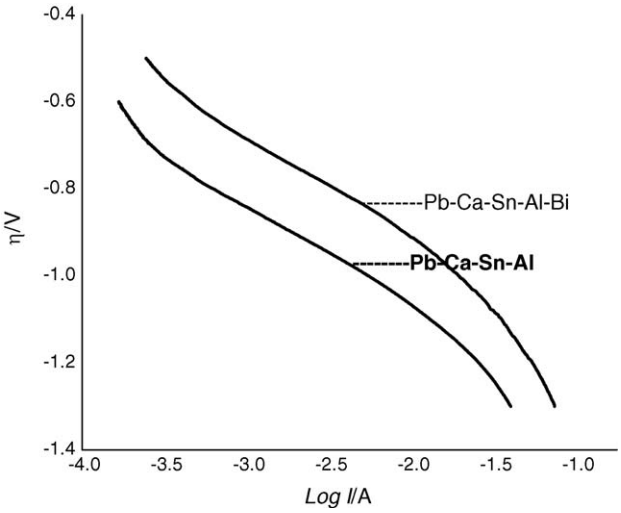

Fig. 13. Tafel curve of over-potential to log *i*.

Table 5
Parameters of Tafel curve of over-potential to log *i*

Electrode	*a*	*b*	*R*
Pb–Ca–Sn–Al–Bi	1.52808	−0.2859	−0.98844
Pb–Ca–Sn–Al	1.60226	−0.2561	−0.98809

$$\eta = a + b \log i$$

Here a is a constant, $b = 2.3RT/\alpha nF$, the Tafel curve is shown as Fig. 13 (Table 5).

The hydrogen evolution current of Pb–Ca–Sn–Al–Bi electrode in 1.65 M H3PO4 was much larger than that of Pb–Ca–Sn–Al electrode. The absolute value of the hydrogen evolution over-potential of Pb–Ca–Sn–Al–Bi electrode was much smaller than that of Pb–Ca–Sn–Al electrode. It indicated the hydrogen evolution easily occurred in Pb–Ca–Sn–Al–Bi electrode.

4. Conclusion

Bismuth in lead alloy electrode could increase the discharge capacity of the electrode in sulfuric and phosphoric acid. The porosity-producing effect of bismuth on the lead alloy electrode leads to the increase of the surface area of electrode, which may play main role in the increase of discharge capacity of alloy electrode in the sulfuric acid solution during cyclic scans.

The oxidation peak potential of lead alloy electrode in phosphoric acid shifted to the positive compared to that in sulfuric acid. The $PbHPO_4$ formed in phosphoric acid will cover the surface of the electrode and lead its passivation, which is responsible for the positive shift of the oxidation. $PbHPO_4$ is a porous material and less compact than $PbSO_4$. As a result, the acidity active material in the plate containing bismuth is higher when the more β-PbO_2 occurs. β-PbO_2 is of tiny crystalline grains with high discharge capacity.

The hydrogen evolution current of Pb–Ca–Sn–Al–Bi electrode in 1.65 M H3PO4. was much larger than that of Pb–Ca–Sn–Al electrode. The absolute value of the hydrogen evolution over-potential of Pb–Ca–Sn–Al–Bi electrode was much smaller than that of Pb–Ca–Sn–Al electrode. It indicated the hydrogen evolution easily occurred in Pb–Ca–Sn–Al–Bi electrode.

References

[1] E. Meissner, J. Power Sources 67 (1997) 135.
[2] S. Tudor, A. Weisstuch, S.H. Davang, Electrochem. Technol. 3 (1965) 90.
[3] S. Tudor, A. Weisstuch, S.H. Davang, Electrochem. Technol. 4 (1965) 406.
[4] K.R. Bullock, D.H. McClelland, J. Electrochem. Soc. 124 (1977) 1496.
[5] K.R. Bullock, J. Electrochem. Soc. 126 (1979) 360.
[6] K.R. Bullock, J. Electrochem. Soc. 126 (1979) 1848.
[7] J. Garche, H. Dōring, K. Wiesener, J. Power Sources 33 (1991) 213.
[8] H. Dōring, K. Wiesener, J. Power Sources 38 (1992) 261.
[9] S. Venugopalan, J. Power Sources 46 (1993) 1.
[10] S. Sternberg, V. Branzoi, L. Apateanu, J. Power Sources (1993) 177.
[11] M. Chatelut, S. Chah-Bouzziri, O. Vittori, A. Benayada, J. Solid State Electrochem. 4 (2000) 435.
[12] I. Paleska, R. Puszkowska-Drachal, J. Kotowski, A. Dziudzi, J.D. Milewski, M. Kopczyk, A. Czerwinski, J. Power Sources 113 (2003) 308.
[13] H.Y. Chen, L. Wu, C. Ren, Q.Z. Luo, X. Jiang, Z.H. Xie, Y.K. Xia, Y.R. Luo, J. Power Sources 4072 (2000) 1.
[14] H.-Y. Chen, Q.-M. Huang, L.-P. Tian, W.-S. Li, J.-L. Tan, Chin. J. Power Sources 5 (2000) 258.
[15] W.-S. Li, H.-Y. Chen, Chin. J. Power Sources 3 (1999) 171.